The Finite Element Analysis of Buckling-Restrained Reduced Beam Section Connections of Steel Frame

C. Y. Liu[1], J. Wu[2], L. Q. Xie[3]

[1] *PhD, the Key Laboratory on Concrete and Prestressed Concrete Structures of Ministry of Education of China, Southeast University, Nanjing, China, liuchenyu0402@163.com*
[2] *Prof., the Key Laboratory on Concrete and Prestressed Concrete Structures of Ministry of Education of China, Southeast University, Nanjing, China, seuwj@seu.edu.cn*
[3] *PhD, the Key Laboratory on Concrete and Prestressed Concrete Structures of Ministry of Education of China, Southeast University, Nanjing, China, seuxlq@seu.edu.cn*

Abstract

Reduced beam section (RBS) connection is one typical type of connection which can move plastic hinge away from the column face by reduction of beam flange adjacent to the beam-to-column connection. However, with the increase of load and cyclic times, the significant out-of-plane buckling may be observed within the reduced region after the flange and web in this region yielding. This phenomenon will strength and stiffness deterioration and adversely affect the seismic performance. In order to solve the problem of local buckling, buckling-restrained reduced beam section (BR-RBS) connection is proposed in which a buckling-restrained device can be installed on the periphery of the reduced region of RBS connection. The significant out-of-plane buckling of flange and web in the reduced region can be effectively limited with this device. In this paper, through the finite element software ABAQUS, two models which include an ordinary RBS connection and BR-RBS connection were built to compare and analysis the effectiveness of this device under cyclic loading. Analysis results show that the device can prevent the strength and stiffness degradation and improve the low-cycle fatigue performance. Excellent energy dissipation capacity and plastic deformation capacity can be obtained.

Keywords: RBS connection; buckling-restrained device; finite element analysis; hysteretic performance

1. Introduction

After the reduced beam section (RBS) beam-to-column moment connection was proposed by Plumier [1], many scholars have conducted a great number of experimental researches and numerical analyses which indicate that RBS can induce plastic hinge formation at an approximate distance from column face and satisfactory plastic deformation capacity and energy dissipation capacity can be obtained [2, 3]. However, with the increase of load amplitude and cycle times, out-of-plane local buckling can be observed with the reduced region after yielding. And the RBS beams are more prone to lateral instability than the ordinary beam which results from the stiffness deterioration due to the flanges reduction. These problems will cause the strength and stiffness degradation of the beam and have an adverse effect on the energy dissipation capacity and low-cycle fatigue performance [4]. In previous study, Nakashima et al. [5] believed that RBS beams can be equipped with necessary lateral bracing just like ordinary beams; the American Institute of Steel Construction Seismic Provisions suggests that additional lateral bracing should be provided in the reduced region, except for the same lateral bracing as ordinary beams. Although the above studies can improve the overall stability of the RBS beams by setting lateral bracing, it is not clear whether the local buckling problem has been alleviated. Li et al. [6] proposed that several stiffeners within the reduced section can be assembled in order to solve the buckling of the flange and web in this region. Saleh et al. [7] proposed a new kind of tubular web RBS (TW-RBS) connection which can improve the overall stability of the beam and delay the occurrence of local buckling in the reduced section due to large out-of-stiffness provided by the tubular web. It can be found according to the above research results that although some measures can be taken to delay the local buckling, local buckling cannot be completely disappeared. A certain degree of buckling will still be observed under large load amplitude which will worsen the seismic performance of the connection. Buckling-restrained brace is a typical type of metal yielding energy dissipation device which can dissipate energy through both tension and compression and has stable hysteretic performance under strong earthquake [8, 9]. Based on the principle of the BRB, a new kind of buckling-restrained reduced beam section (BR-RBS) connection is proposed in this paper in which the buckling-restrained device arranged in the reduced region can limit the buckling of the flange and web and provide enough out-of-plane stiffness to improve the overall stability of the beam. Therefore, the strength and stiffness deterioration can be prevented and excellent energy dissipation capacity and plastic deformation capacity can be obtained with the BR-RBS. In this paper, the construction of the proposed connection is introduced in detail and finite element analysis is conducted to analyze the mechanical properties of this connection under cyclic loading. The effectiveness of this buckling-restrained device is verified in comparison with ordinary RBS connection.

2. The construction of the BR-RBS connection

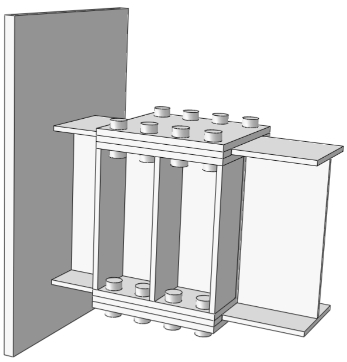

Fig. 1 – Construction of BR-RBS connection

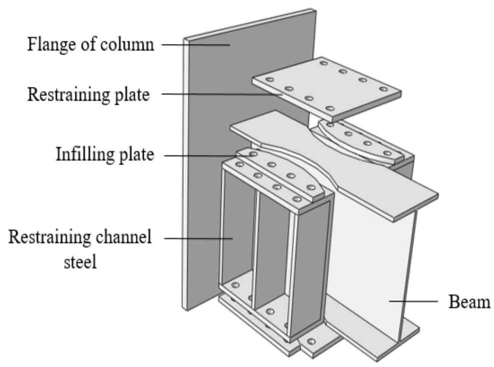

Fig. 2 – Components of BR-RBS connection

The construction of the proposed BR-RBS connection in this paper is provided in Fig.1. The buckling-restrained device mainly consists of two restraining plates, two restraining channel steels and four infilling plates, which are connected by high-strength bolts, as shown in Fig.2. The specific construction methods of the buckling-restrained device are as follows: ①The buckling-restrained device should maintain elasticity and avoid the overall instability when limiting the buckling of the core plate. Therefore, sufficient bending stiffness of the restrained plate should be guaranteed. ②The infilling plates can prevent the movement of the buckling-restrained device along the length of the beam. The shape of the infilling plate near the beam flange is consistent with the reduction shape. ③In order to ensure that enough space can be provided for the deformation of the beam due to Poisson effect under compression and the low-cycle fatigue performance of the reduced region cannot be deteriorated [10], appropriate clearance should be reserved between the restrained components and the beam. Unbonded material can be pasted in the clearance for the purpose of reducing the friction. ④The constraint range of the device should not be less than the length of the flange reduction. Additionally, the three weakening parameters of the RBS beam as shown in Fig.3 can be evaluated according to FEMA-350 [11], namely: a = (0.50~0.75) b_f, b = (0.65~0.85) h_b, c = (0.20~0.25) b_f. Where, b_f is the width of the beam flange and h_b is the height of beam section.

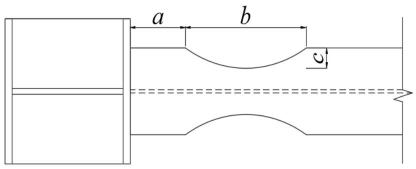

Fig. 3 – Weakening parameters of RBS connection

3. Numerical study

ABAQUS computer program was used to analyze the seismic performance of the ordinary RBS connection and the new BR-RBS connection under cyclic loading. Except that the BR-RBS connection has a buckling-restrained device in the reduced region, all other parameters including geometric parameters, material properties and boundary conditions remain the same towards the two connections.

HN300×150×6.5×9 and HW400×400×13×21 hot-rolled H-beam were selected for the beams and columns of both connections, respectively. The geometric dimensions in detail are presented in Fig.4. The restraint range of the device is the same as the length of the flange reduction, which is 240 mm. The thickness of steel plate of the restraining plate and restraining channel steel is 16 mm, and the thickness of the infilling plate is 11 mm. A 1mm clearance is maintained between each restrained component and the beam.

The material selected in the finite element analysis is Q345B steel. The mechanical performance parameters of this kind of material are as follows: yielding strength σ_y = 345 MPa, Young's modulus E = 205 GPa, Poisson's ratio v = 0.3. A combined (isotropic–linear kinematic) hardening rule with a Von Mises yielding criterion is used to describe the nonlinear behavior of materials after yielding [12].

The plastic deformation requirements of the welds at the beam-to-column connection can be reduced with the RBS connection, thus, the simulation of weld performance can be ignored. The "tie" constraint is used to connect the beam and column. In addition, with regard to the buckling-restrained device, the contact surfaces between each restraint component are bound together with "Tie" constraint regardless of the influence of bolts. Tangential and normal contacts are considered between each component of the device and the beam.

The boundary conditions of the analytical connections are shown in Fig.5. The top and bottom of the column are set with hinged constraints. The lateral instability of the beam is restricted at a distance of 1 m from the column face. Moreover, all the nodes of the beam free end section are coupled by Y-direction displacement, and the loading is applied to the main node of the coupling surface. A cyclic displacement history with increasing amplitude was imposed to the beam free end step by step, as shown in Fig.6. The displacement amplitudes were obtained from the objective story drift of each step. The story drift is the ratio between the beam free end displacement and the distance between the loading position and the column face (L=1500 mm). The increasing story drifts were chosen as 0.25%, 0.5%, 1.0%, 1.5%, 2.0%, 2.5%, 3.0%, 3.5%, 4.0%, 4.5%, 5.0%, 5.5% and 6.0%, respectively, while the beam free end displacements were chosen as 3.75 mm, 7.5 mm, 15 mm, 22.5 mm, 30 mm, 37.5 mm, 45 mm, 52.5 mm, 60 mm, 67.5 mm, 75 mm, 82.5 mm and 90 mm, respectively. The story drifts of 0.25%~1.0% experienced 3 cycles at each amplitude, while the drifts of 1.5%~3.0% experienced 2 cycles, and the other drifts experienced 1 cycle.

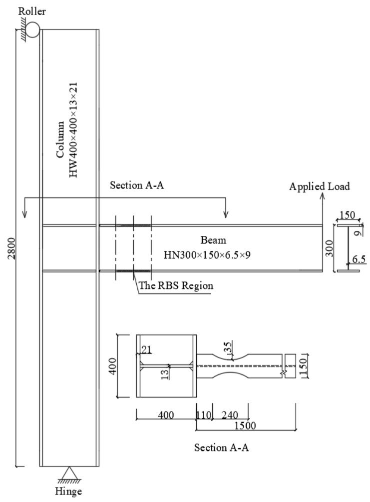

Fig. 4 – Details of RBS connection

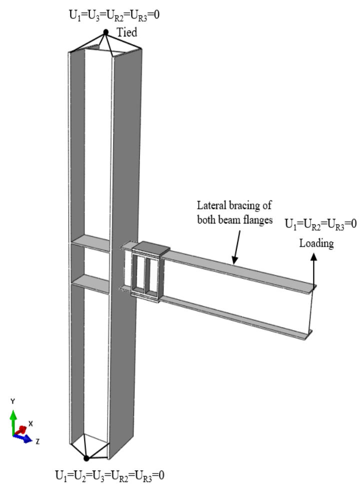

Fig. 5 – Boundary conditions

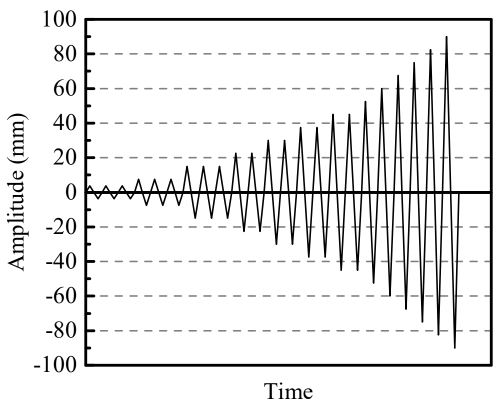

Fig. 6 – Loading protocol

Eight-node solid elements with reduced integration techniques (C3D8R) are used to model the two connections. Each node of this element has three translational degrees of freedom in the xyz direction, and material plasticity, stress strengthening and large deformation can be considered by using this element. In order to improve the calculation efficiency, gird refinement was carried out for the reduced region and the region of the beam end, and the regions far away from the beam-to-column connection were divided with a larger grid size under the premise of ensuring sufficient calculation accuracy, as shown in Fig.7.

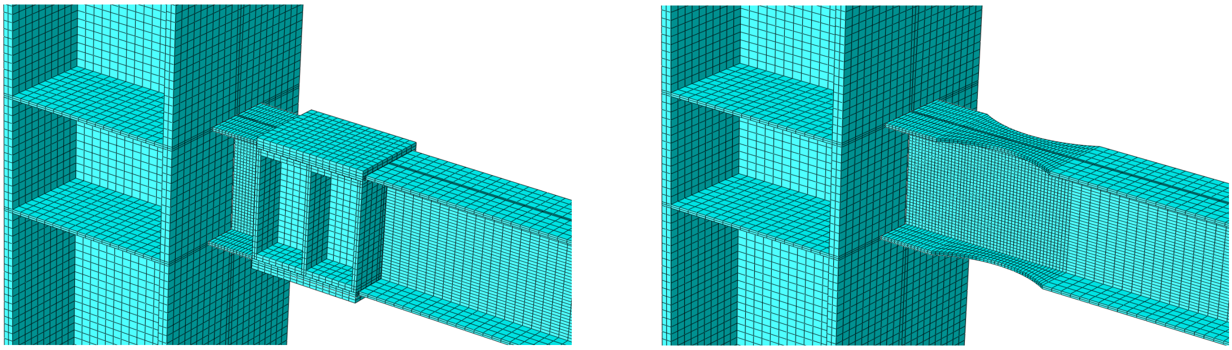

(a) RBS (b) BR-RBS

Fig. 7 – Finite element models

4. Description of model analysis

4.1 Failure process

The RBS connection remained elastic during the cycles of 0.25%~0.5% story drift. The maximum stress and strain in the RBS beam occurred at the center of the reduced region where the flange width in this region is minimal. After the beam flange yielded (after 1.0% story drift), the plastic region of the flange in the reduced section expanded continuously. Additionally, plastic region was also discovered at the top and bottom sides of the web in this region. At 2.5% story drift, total cross-section of the web exceeded the yielding strength. At the same time, the flange had been strengthened at the center of the reduced region. Therefore, the plastic hinge had been formed in this region. Slight buckling was observed at the top and bottom reduced flange during the second cycle of 2.5% story drift. The deformed shape and strain distribution along the beam length at 2.5% story drift is provided in Fig.8. Thereafter, with the increase of displacement amplitude, the local buckling in the reduced region became more and more serious, and obvious bulging of the web was also observed. The position of the beam with the maximum stress and strain was concentrated in the region where the buckling was the most serious, which caused the plastic hinge was not fully developed. Moreover, on account of the low out-of-plane stiffness after bucking, the lateral torsional instability of the beam occurred. As illustrated in Fig.9, during 6.0% story drift, the maximum Von Mises stress of the beam flange had exceeded 600 MPa, and the strain along the beam length was close to 25% due to severe buckling in the reduced region. As a consequence, the connection had failed due to the steel fracture.

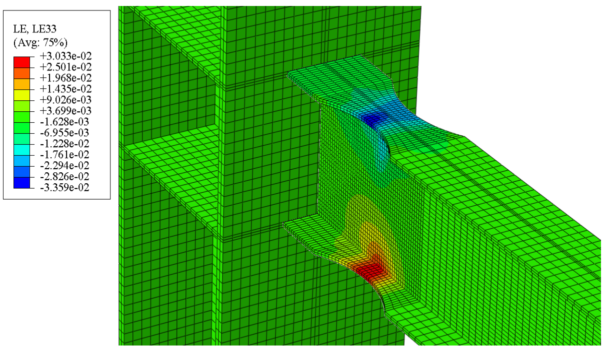

Fig. 8 – Deformed shape and strain distribution of RBS at 2.5% story drift

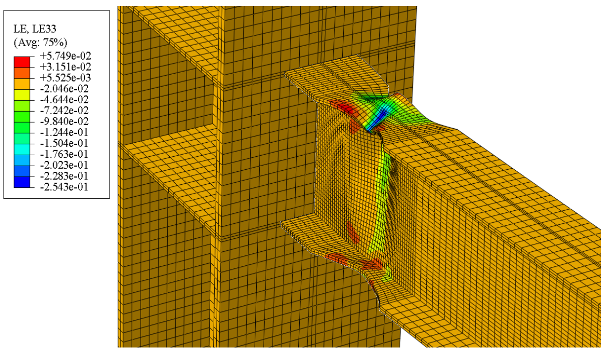

Fig. 9 – Deformed shape and strain distribution of RBS at 6.0% story drift

For the BR-RBS connection, before the cycles of 2.5% story drift, there was no local buckling in the reduced region, thus, the buckling-restrained device did not contact with the beam. The stress and deformation of the BR-RBS connection were consistent with that of the ordinary RBS connection. During the second cycle of 2.5% story drift, when the local buckling of the reduced flange was discovered, the buckling-restrained device began to work. The normal stress with small value appeared on the device due to the mutual extrusion between the device and the beam. During the subsequent loading process, the local buckling of the reduced region was effectively limited by the device, and the plastic hinge region was fully developed compared with the ordinary RBS connection. Thus, the energy dissipation energy of this kind of connection was greatly improved. The deformed shape and strain distribution along the longitudinal direction of the beam at 6.0% story drift is presented in Fig.10. It can be seen from this figure that the problem of local buckling was well improved. However, because there was a 1 mm gap between the device and the beam, the flange and web in the reduced region would still slightly buckle within this clearance at large story drift. According to Fig.11 which shows the Von Mises stress distribution of the buckling-restrained device at 6.0% story drift, the maximum Von Mises stress was 160 MPa which indicates that the device remained elastic during the whole loading process. Moreover, there was no overall torsional instability of the BR-RBS beam after the entire loading process.

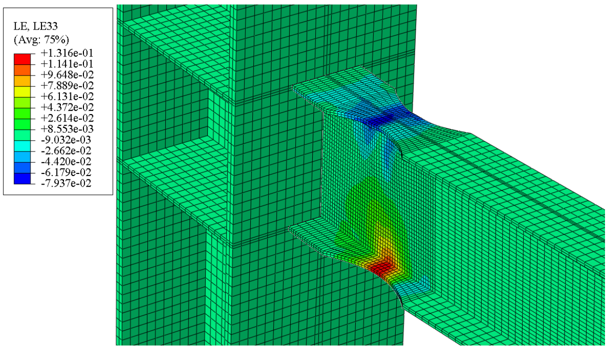

Fig. 10 – Deformed shape and strain distribution of BR-RBS at 6.0% story drift

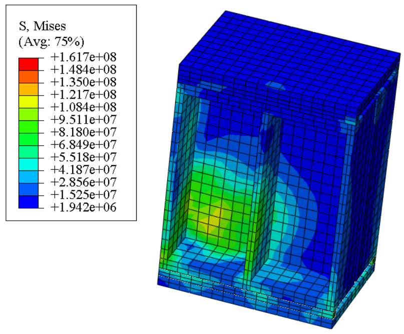

Fig. 11 – Von Mises stress distribution of buckling-restrained device at 6.0% story drift

4.2 Strain distribution

In order to analyze the stress state of these two connections under different displacement amplitude, as shown in Fig.12, a longitudinal path of the beam flange named Path1 was set, which starts from the midpoint of the beam flange end. With the increasing of the distance from beam-to-column connection, the stress on the beam flange will decrease obviously. Only the length range of 350 mm from the beam-to-column connection was selected for the study, including the reduced region and the beam flange end. The strains along the beam length on Path1 were extracted from the results of the finite element analysis. In this paper, the strain value is positive under compression and negative under tension.

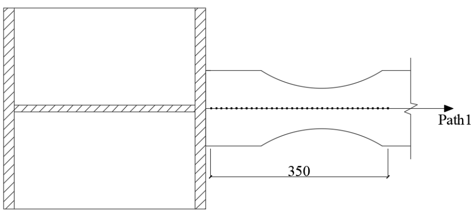

Fig. 12 – Analytic path on beam flange

Fig.13 shows the strain distribution curves of the two connections on Path1 under different story drift amplitude. It can be found that before the local buckling occurred at 2.5% story drift, the strain distribution on the beam flange of the two connections at the same amplitude is similar. The position with the maximum strain value on the flange is the center of the reduced region which has the minimum flange width. During the cycles of 1.0% story drift, the flange at the center of the reduced section yields, after which the stress grows slowly, while the strain develops rapidly. A certain degree of plastic strain concentration appears at this position. The plastic region of the flange expands continuously with the increase of story drift amplitude, and the flange near the center of the reduced region has been strengthened at 2.5% story drift, which leads to a plastic hinge forming at this position.

Slight buckling of the ordinary RBS connection was observed during the second cycle of 2.5% story drift, and the buckling became more serious with the story drift amplitude. It can be found from Fig. 13a that the strain near the center of the reduced region exhibits a significant increase after the cycles of 2.5% story drift. And at 6.0% story drift, the strain at this position is close to 25% which reaches the ultimate strain of the steel, therefore, the steel in the reduced region has undergone low-cycle fatigue fracture. However, during 2.5% and the subsequent story drift cycles, the strain in the reduced region of the BR-RBS connection maintains a stable growth without sharp increase due to the fact that the buckling was limited by the device. The strain in the reduced region of the new kind connection is smaller than that of RBS connection at the same story drift, and the strain along the beam length in the reduced section is close to 7.0% during 6.0% story drift. It can be concluded that the strain level in the reduced region can be effectively decreased with the buckling-restrained device which indicates the low-cycle fatigue performance of the connection can be improved. In addition, compared with the RBS connection, the plastic hinge of the reduced region of the BR-RBS connection develops more fully during the whole loading process, thus, the energy dissipation capacity is more excellent.

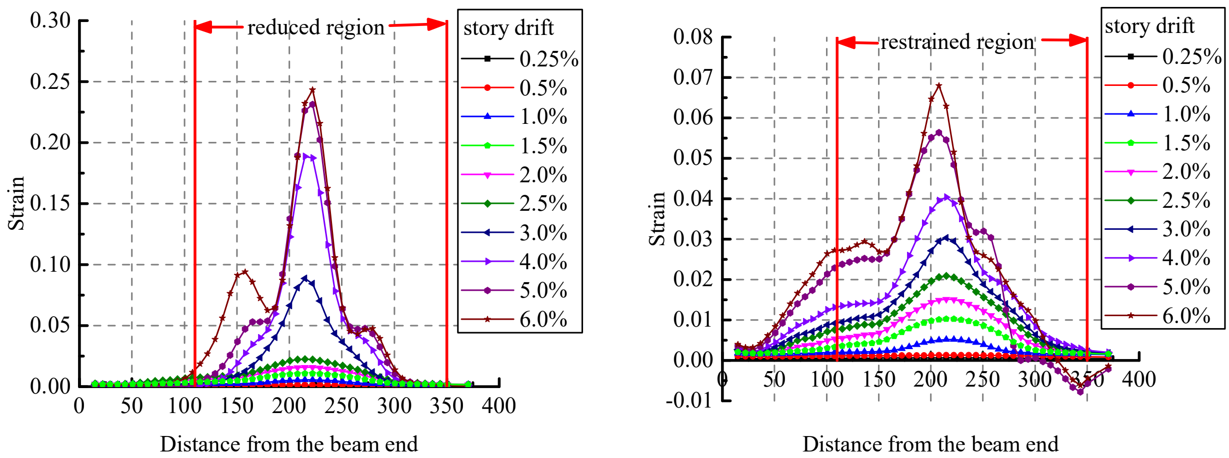

(a) RBS (b) BR-RBS

Fig. 13 – Strain distribution curves on Path 1

4.3 Hysteretic property

The load-displacement curves which are plump spindle-shaped curves at the loading point for the two connection are shown in Fig.14. Before 2.5% story drift, the two hysteretic curves are similar. The force of the RBS connection gradually decreases after 2.5% story drift. Obvious deterioration of the strength and stiffness is observed owing to the fact that serious local buckling in the reduced region and lateral buckling of the beam occurred with the increase of load and cyclic times. On the contrary, similar problems did not appear during the whole loading process on BR-RBS connection. The force of the BR-RBS connection shows a stable increase with the story drift amplitude after the reduced region is strengthened. It is clear that the buckling-restrained device can prevent the degradation of the strength and stiffness of the RBS connection. The energy dissipation capacity of this kind of BR-RBS connection is more excellent than that of ordinary RBS connection.

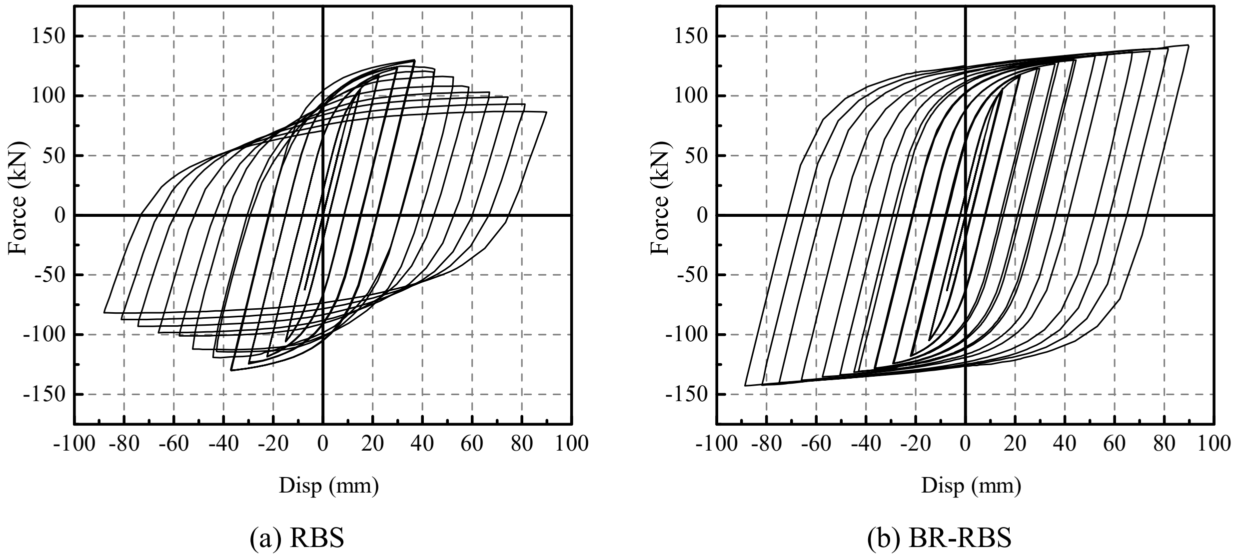

Fig. 14 – Load-displacement curves for the connections

4.4 Skeleton curves

The skeleton curves of these two connections are provided in Fig.15. Before the local buckling of the RBS connection occurred, there is no significant difference in stiffness between the BR-RBS connection and RBS connection. The skeleton curves of the connections are symmetrical in the stages of the positive and negative loading. The force of the RBS connection reaches the limit at 2.5% story drift and decreases to 85% of the limit during the cycle of 4.0% story drift which reveals that the connection has failed. No decrease of the force of the BR-RBS connection is observed during the whole loading process. After the reduced flange yields, the connection stiffness becomes smaller and the skeleton curve tends to be flat. The bearing capacity also shows a certain increase, which is mainly due to the strengthening of the reduced region after yielding. No negative stiffness emerges during the loading process, that is, the stiffness after yielding is stable. Therefore, the skeleton curve of the BR-RBS connection can be simplified as a conduplicate-line.

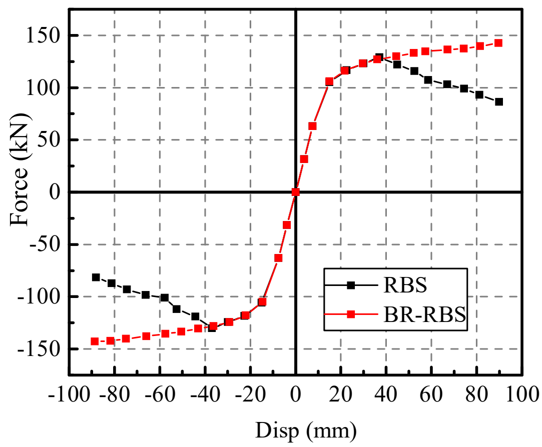

Fig. 15 – Skeleton curves

The mechanical properties of the two connections according to the skeleton curves are listed in Table 1. It can be seen that the ratio between the maximum and yielding loads (F_m/ F_y) of the RBS connection and BR-RBS connection on the beam free end according to the finite element analysis is 1.20 and 1.32, respectively. Compared with RBS connection, BR-RBS connection has higher bearing capacity and safety reserve.

Table 1 – Mechanical properties of the connections

Connection	F_y (kN)	F_m(kN)	F_m/ F_y	Δ_y(mm)	Δ_m (mm)	Δ_m/Δ_y
RBS	107.80	129.03	1.20	16.78	56.88	3.39
BR-RBS	107.80	142.50	1.32	16.78	90.00	5.36

Note: F_y is the yielding force of the connection; Δ_y is the yielding displacement at the beam free end; F_m is the ultimate force of the connection; Δ_m is the ultimate displacement at the beam free end.

4.5 Ductility

As shown in Table 1, the ratio between the maximum displacement and the yielding displacement (Δ_m/ Δ_y) for connection BR-RBS and RBS is 3.70 and 4.53, respectively. The ultimate load of the BR-RBS connection is greatly improved compared with the RBS connection, thus, the ultimate displacement increases. Better plastic deformation capacity can be obtained with the BR-RBS connection.

5. Conclusions

The finite element software ABAQUS was used to analyze the BR-RBS connection proposed in this paper and ordinary RBS connection under cyclic loading. The failure process, ductility, bearing capacity and hysteretic performance of each connection were obtain from the finite element analysis. The strain distribution in the reduced region was also studied. The main conclusions are as follows:

1) The bearing capacity and stiffness of the RBS connection are significantly degraded due to severe local buckling in the reduced region. Under large displacement amplitude, the hysteretic curve is not very plump, which has an adverse effect on the energy dissipation capacity of the connection.

2) The buckling-restrained device can effectively decrease the strain level in the reduced region, which reveals that excellent low-cycle fatigue performance can be obtain with this kind of device.

3) BR-RBS connection show no deterioration of the strength and stiffness during the whole loading process compared with the RBS connection. Excellent plastic deformation capacity and energy dissipation capacity can be obtained by using the BR-RBS connection.

6. Acknowledgements

The authors would like to acknowledge financial support from the China National Key Research and Development Program (2016YFC0701403), the National Natural Science Foundation of China (51278105), and the Priority Academic Program Development of Jiangsu Higher Education Institutions (PAPD).

7. Copyrights

8. References

[1] Plumier A (1997): The dog bone: Back to the future. *Engineering Journal*, **34** (2), 61-67.

[2] Jones SL, Fry GT, Engelhardt MD (2002): Experimental evaluation of cyclically loaded reduced beam section moment connections. *Journal of Structural Engineering*, **128** (4), 441-451.

[3] Zhang XF, Ricles JM (2006): Seismic behavior of reduced beam section moment connections to deep columns. *Journal of Structural Engineering*, **132** (3), 358-367.

[4] Yu YS, Wang Y (2009): Experimental study on the mechanical property of reduced beam section connections of steel frames. Engineering mechanics, **26** (2), 168-175. (in Chinese)

[5] Nakashima M, Kanao I, Liu D (2002): Lateral instability and lateral bracing of steel beams subjected to cyclic loading. *Journal of Structural Engineering*, **128** (10), 1308-1316.

[6] Li F, Kanao I, Li J (2009): Local buckling of RBS beams subjected to cyclic loading. *Journal of Structural Engineering*, **135** (12), 1491-1498.

[7] Saleh A, Mirghaderi SR, Zaharai SM (2016): Cyclic testing of tubular web RBS connections in deep beams. *Journal of Constructional Steel Research*, **117**, 214-226.

[8] Wu J, Liang RJ, Wang CL, Ge HB (2012): Restrained buckling behavior of core component in buckling-restrained braces. *Advanced Steel Construction*, **8** (3), 212-225.

[9] Xie LQ, Wu J, Huang Q (2018): Experimental study on low-cycle fatigue performance of weld-free buckling-restrained braces. *Journal of Earthquake Engineering*, **22** (8), 1392-1414.

[10] Huang Q (2013): Low-cycle fatigue performance and seismic demands of welding-free buckling-restrained braces. Southeast University, Nanjing, China. (in Chinese)

[11] Federal Emergency Management Agency (2000): Recommended seismic design criteria for new steel moment-frame buildings. *FEMA-350*, Washington DC, USA.

[12] Shi YJ, Wang M, Wang YQ (2012): Experimental study of structural steel constitutive relationship under cyclic loading. Journal of Building Materials, **15** (3), 293-300. (in Chinese)